Received: 29 April 2016 | Revised: 14 August 2017 | Accepted: 15 August 2017

DOI: 10.1002/jnm.2298

EMF 2016 SYMPOSIUM

WILEY

Nodal discontinuous Galerkin method for high-temperature superconductors modeling based on the H-formulation

L. Makong[1,2] | A. Kameni[1] | F. Bouillault[1] | C. Geuzaine[3] | P. Masson[2]

[1]Group of electrical engineering Paris, UMR 8507 CNRS, CentraleSupelec, Université Paris Sud, Université Pierre et Marie Curie, Paris, France,

[2]Department of Mechanical Engineering, University of Houston, Houston, TX 77204, USA

[3]Department of Electrical Engineering and Computer Science, Montefiore Institute Sart-Tilman, Université de Liège, Liège 4000, Belgium

Correspondence
L. Makong, Department of Mechanical Engineering, University of Houston, Houston, TX 77204, USA.
Email: lmakonghellnkatack@uh.edu

Abstract

There is growing interest in superconducting machinery design in AC regime such as generators, motors, and magnets. High-temperature superconductors are used as tapes or cables for the machine windings. Therefore, AC losses have to be evaluated efficiently for an optimal design. Moreover, non-linearities, arising from the power law characterizing the electrical behaviour of superconductor, have to be also dealt with. The development of efficient numerical methods is therefore critical to model high-temperature superconductors. Although numerous methods have already been proposed, the finite element method applied on the time-dependent curl-curl–based **H**-formulation remains the mostly used. It uses edge elements of Nedelec to naturally ensure the continuity of the tangential components of **H**. To take into account non-linearities from superconductors, a linearisation of the superconductors constitutive power law $\mathbf{E} = \rho(\mathbf{J})\mathbf{J}$ was implemented. Discontinuous Galerkin finite element method provides an interesting alternative to edge elements for the time-dependent **H**-formulation. Indeed, the curl-curl operator is written as a div operator and the interior penalty approach defines numerical fluxes at the interfaces. Those fluxes will ensure the continuity of the tangential components of **H**. The resistivity $\rho(\mathbf{J})$ is explicitly evaluated at the previous iteration with such an approach leading to convergence. In this paper, both numerical approaches implementation will be presented. We will also compare the numerical results from those methods applied to 3*D* modelling of simple superconducting geometries in AC regime.

KEYWORDS

discontinuous Galerkin method, high-temperature superconductors, Maxwell equations

1 | INTRODUCTION

The development of high-temperature superconductors (HTS) is generating a growing interest in several superconductivity applications such as motors design for aircraft propulsion[1] and magnets design for medical imaging.[2] Those applications, mostly alternating, require superconductors because they can carry high currents thus they can produce high magnetic fields. The resulting AC losses, as one of the main design criteria, must be evaluated accurately and reduced as much as possible by appropriate methods. The efficient evaluation of the AC losses must take in account the highly non-linear electrical behaviour characterizing high-temperature

superconductors and described by the constitutive power law.[3] Complexities arising from the geometry and the external magnetic field configurations must also be considered.

Thus, efficient numerical tools must be developed to model high-temperature superconductors in 3*D* and evaluate accurately resulting AC losses. Different formulations, such as the **H**-formulation, mostly using the conventional finite element method, have been investigated and validated.[4,5] However, the high number of degrees of freedom coupled with the non-linearities associated with the constitutive power law generally slow the convergence leading to computation time varying from hours to days.[6]

The discontinuous Galerkin (DG) method,[7] which is natural for parallel computations, might provide a framework with numerous possibilities. With advanced developments, like GPU computations, the framework might also potentially be geared for fast and efficient computations of superconductivity problems in 3*D*. In such framework, the problem is locally solved on each element of the meshed domain rendering the method scalable over numerous processors without accuracy loss. Unlike the finite element method, computations of large-scale problems, using the discontinuous Galerkin method, are done with no memory limitations due to the meshed domain size.

The method has successfully been applied, in previous works related to the 3*D* modeling of superconductors, for solving the non-linear formulation based on the electric field **E**.[8,9] Despite the efficiency and robustness of this approach for anisotropic and heterogeneous domains, the evaluation of the total magnetic field at the outside boundaries requires the knowledge of the demagnetization coefficients. Complexities of modeled geometries, in the case of twisted tapes or multi-filamentary wires, will likely limit such knowledge.

Thus, we investigate, in this paper, a nodal discontinuous Galerkin method based on the **H**-formulation. To compute the right magnetic field in the studied domain, an appropriate magnetic field will be imposed on the external boundary of an air region surrounding the superconducting system. Moreover, a symmetry interior penalty method, inspired by the work of Grote,[10] will be used to ensure the continuity of the tangential component of the magnetic field.

Comparisons will be made between the numerical implementation of the **H**-formulation using the discontinuous Galerkin method and the finite element method implemented in the software GetDP.[11]

Two simple applications, a superconducting cube and a superconducting wire inside a resistive matrix both subjected to an external alternating magnetic field, will be modeled in 3*D* to validate the proposed method. In each application, the computed AC losses will be compared for both methods.

2 | PROBLEM FORMULATION

2.1 | Domain definition

The studied problem is formulated on a global domain Ω. It generally includes a superconducting sub-domain Ω_s and a non-superconducting sub-domain Ω_r which are both non-overlapping. In multi-filamentary superconducting wire for instance, the superconducting domain can represent all the filaments while the non-superconducting domain includes both the resistive matrix and the air domain around the wire.

The magnetic and electrical behaviour of the domain Ω are generally defined by each of the following Equations 1 and 2:

$$\mathbf{B} = \mu_0 \mathbf{H}, \tag{1}$$

$$\mathbf{E} = \rho \mathbf{J}, \tag{2}$$

with $\mathbf{B}$ the magnetic flux density, $\mathbf{H}$ the magnetic field, μ_0 the free space's permeability, $\mathbf{E}$ the electric field, $\mathbf{J}$ the current density, and ρ the resistivity.

Moreover, the characterized non-linear electrical behaviour of superconductors suggests a non-linear resistivity describing the superconducting sub-domain Ω_s. This non-linear characteristic is derived from a power law.[3] Thus, the domain resistivity ρ will be defined as follows:

$$\rho = \begin{cases} \rho_s = \frac{E_c}{J_c} \left\| \frac{\mathbf{J}}{J_c} \right\|^{n-1} \text{ in } \Omega_s \\ \rho_r \text{ in } \Omega_r \end{cases} \tag{3}$$

with the non-superconducting sub-domain resistivity ρ_r assumed constant. The quantities E_c, J_c and n are the critical electric field, the critical current density, and the power law exponent associated with the power law.

2.2 | Differential formulation

The **H**-formulation results from the coupling of Maxwell's equations and the constitutive equations described above. The non-linear vectorial equation obtained is the following:

$$\mu_0 \frac{\partial \mathbf{H}}{\partial t} + \text{curl}(\rho \cdot \text{curl}\mathbf{H}) = \mathbf{0}. \tag{4}$$

According to the same Maxwell's equations, while the magnetic field $\mathbf{H}$ is expected to have its normal component continuous at the domain's interfaces, the tangential component will be discontinuous if there is a surface current at the interfaces. However, surface currents are assumed negligible leading to the continuity of the tangential component of $\mathbf{H}$ at the domain's interfaces.

The exterior domain $\partial\Omega = \Gamma$ will generally include a set of Dirichlet boundaries $\Gamma^{\mathcal{D}}$ and a set of Neumann boundaries $\Gamma^{\mathcal{N}}$ such that $\Gamma = \Gamma^{\mathcal{D}} \cup \Gamma^{\mathcal{N}}$ with $\Gamma^{\mathcal{D}} \cap \Gamma^{\mathcal{N}} = \emptyset$.

On Dirichlet boundaries, the equivalent external magnetic field $\mathbf{H_a}$ around the studied domain Ω, transport current included, will be imposed. Those boundaries belong to the air sub-domain or a sub-domain whose resistivity is as high as the air resistivity. Neumann boundaries, typically associated with symmetry or infinite conditions, have non-zero current.

2.3 | Variational formulation

To solve the non-linear vectorial equation (4), a variational formulation must be derived regardless of the numerical approach used. A first step in this process consists in finding the unknown field $\mathbf{H} \in (\mathbf{L}^2(\Omega))^3$ such that

$$\int_\Omega \frac{\partial \mathbf{H}}{\partial t} \cdot \boldsymbol{\varphi} d\Omega + \int_\Omega \text{curl}(\kappa \cdot \text{curl}\mathbf{H}) \cdot \boldsymbol{\varphi} d\Omega = \mathbf{0}, \quad \forall \boldsymbol{\varphi} \in (\mathbf{L}^2(\Omega))^3 \tag{5}$$

with $\kappa = \rho/\mu_0$ and $\boldsymbol{\varphi}$ the basis vector function. The general solution space of the unknown field $\mathbf{H}$, defined above, will be restricted based on both the chosen numerical approach and the physics.

A numerical approach, implemented on the finite element software GetDP, is publicly available and geared towards superconductors modeling. However, this approach is not yet adapted for large-scale applications because it has not been optimized for parallel computations. Thus, a nodal discontinuous Galerkin method is proposed because it provides more flexibility in terms of parallel computations.

The discrete variational formulation and the non-linearities treatment implemented in both approaches will be discussed. To validate the proposed method, comparisons of both approaches applied to simple superconductivity applications will be done.

3 | FINITE ELEMENT METHOD

The numerical approach implemented to solve the $\mathbf{H}$-formulation in the finite element software GetDP will be presented. The treatment of non-linearities, arising from the power law describing the electrical behaviour of superconductors, will also be discussed.

We will first define the discretization of Ω and the associated finite element spaces to derive the discrete weak formulation resulting from the $\mathbf{H}$-formulation.

3.1 | Mesh definition

Let us consider a three-dimensional conforming mesh $\mathcal{T}_h$, which is a partition of the domain Ω in tetrahedral or hexahedral elements K such that $\Omega = \cup_{K \in \mathcal{T}_h} K$. The size of each element is denoted by h_K. We assume that the mesh is aligned with the discontinuities of the material properties, such as the resistivity ρ, present in the domain. Therefore, $\mathcal{T}_h = \mathcal{T}_{h,s} \cup \mathcal{T}_{h,r}$ with $\mathcal{T}_{h,s}$ and $\mathcal{T}_{h,r}$, respectively, representing the meshes of the sub-domains Ω_s and Ω_r.

All the faces of the mesh $\mathcal{T}_h$ belong to the set $\Gamma_h = \Gamma_h^{\mathcal{I}} \cup \Gamma_h^{\mathcal{B}}$, where $\Gamma_h^{\mathcal{I}}$ is the set of all the interior faces and $\Gamma_h^{\mathcal{B}}$ the set of the boundary faces.

Among the boundary faces, there will be faces with either Dirichlet or Neunmann boundary conditions such that $\Gamma_h^{\mathcal{B}} = \Gamma_h^{\mathcal{B},\mathcal{D}} \cup \Gamma_h^{\mathcal{B},\mathcal{N}}$. $\Gamma_h^{\mathcal{B},\mathcal{D}}$ is the set of boundary faces with Dirichlet conditions while $\Gamma_h^{\mathcal{B},\mathcal{N}}$ is the one with Neumann conditions.

3.2 | Discrete variational formulation

The finite element discretization of Equation 4 will need an approximation of the unknown magnetic field $\mathbf{H}$ based on Nedelec elements. The approximated field $\mathbf{v}^h$ will be defined over the mesh $\mathcal{T}_h$. It will belong to the following finite element space:

$$\mathbf{V}^h = \left\{ \mathbf{v} \in H(\text{curl};\ \Omega) : \mathbf{v}|_K \in (\mathbb{P}^1(K))^3, K \in \mathcal{T}_h \right\} \tag{6}$$

with

$$H(\text{curl};\ \Omega) = \left\{ \mathbf{v} \in (\mathbf{L}^2(\Omega))^3 : \text{curl}\mathbf{v} \in (\mathbf{L}^2(\Omega))^3 \right\}. \tag{7}$$

The discrete weak formulation of Equation 4 will consist in finding $\mathbf{v}^h \in \mathbf{V}^h$ such that

$$\begin{aligned} &\int_{\mathcal{T}_h} \mathbf{v}_t^h \cdot \boldsymbol{\varphi} d\mathcal{T}_h + \int_{\mathcal{T}_h} \kappa \cdot \text{curl}\mathbf{v}^h \cdot \text{curl}\boldsymbol{\varphi} d\mathcal{T}_h \\ &\quad - \int_{\Gamma_h^{\mathcal{B},\mathcal{N}}} ((\kappa \cdot \text{curl}\mathbf{v}^h) \times \mathbf{n}) \cdot \boldsymbol{\varphi} dA + I_h^{\mathcal{B},\mathcal{D}} \\ &\quad = \mathbf{0}, \quad \forall \boldsymbol{\varphi} \in \mathbf{V}^h \end{aligned} \tag{8}$$

with $\mathbf{v}_t^h = \partial \mathbf{v}^h / \partial t$, $\kappa = \rho/\mu_0$ and $I_h^{\mathcal{B},\mathcal{D}} = \int_{\Gamma_h^{\mathcal{B},\mathcal{D}}} \boldsymbol{\lambda} \cdot \boldsymbol{\varphi} dA + \int_{\Gamma_h^{\mathcal{B},\mathcal{D}}} (\mathbf{v}^h - \mathbf{H_a}) \cdot \boldsymbol{\lambda}' dA$.

The Lagrange coefficients $\boldsymbol{\lambda}$ and $\boldsymbol{\lambda}'$ help impose the Dirichlet boundary conditions in a weakly way. They also belong to the finite element space $\mathbf{V}^h$.

3.3 | Numerical treatment of the non-linearities arising from $\mathbf{E} = \rho(\mathbf{J})\mathbf{J}$

The electrical behaviour of the superconducting domain Ω_s is defined by a non-linear power law as shown in (2) and (3).Therefore, the discrete variational formulation, expressed in (2), must take in account those non-linearities.

At each time step t_p^l of the problem resolution, the power law will be approximated by a first-order Taylor expansion.

A Newton-Raphson algorithm will ensure that convergence is reached for a good power law approximation. The linearised power law at the iteration k of the Newton Raphson algorithm is the following:

$$\mathbf{E}(\mathbf{J}_k) = \mathbf{E}(\mathbf{J}_{k-1}) + \overline{\overline{\mathbf{A}}} \cdot (\mathbf{J}_k - \mathbf{J}_{k-1}) \tag{9}$$

with

$$\begin{aligned}\overline{\overline{\mathbf{A}}} &= A_{ij} = \partial E_i / \partial J_j \\ &= \begin{cases} \dfrac{(n-1)E_c}{J_c^n} J_i^2 \|\mathbf{J}\|^{n-3} + \dfrac{E_c}{J_c^n}\|\mathbf{J}\|^{n-1} & , i = j \text{ in } \Omega_s \\ \dfrac{(n-1)E_c}{J_c^n} J_i J_j \|\mathbf{J}\|^{n-3} & , i \neq j \text{ in } \Omega_s \\ \rho_r & , i = j \text{ in } \Omega_r \\ 0 & , i \neq j \text{ in } \Omega_r \end{cases}\end{aligned} \tag{10}$$

where $i,j = 1, 2$, and 3. Moreover, the current density $\mathbf{J}_{k-1}$and the corresponding electric field, evaluated at the iteration k-1 of the Newton-Raphson algorithm, are known. The power law linearisation will be formulated directly in the discrete variational formulation as an approximation of the following volumic term of the superconducting domain:

$$\int_{\mathcal{T}_{h,s}} \kappa \cdot \mathrm{curl}\mathbf{v}_k^h \cdot \mathrm{curl}\, \boldsymbol{\varphi} d\mathcal{T}_{h,s} \tag{11}$$

The approximated expression of (11), based on the power law linearisation, will give

$$\begin{aligned}&\int_{\mathcal{T}_{h,s}} \kappa_{k-1} \cdot \mathrm{curl}\mathbf{v}_{k-1}^h \cdot \mathrm{curl}\boldsymbol{\varphi} d\mathcal{T}_{h,s} \\ &\qquad + \mu_0^{-1} \int_{\mathcal{T}_{h,s}} \overline{\overline{\mathbf{A}}} \cdot (\mathrm{curl}\mathbf{v}_k^h - \mathrm{curl}\mathbf{v}_{k-1}^h) \cdot \mathrm{curl}\boldsymbol{\varphi} d\mathcal{T}_{h,s}.\end{aligned} \tag{12}$$

In the numerical implementation, we noticed that the defined tensor A_{ij} ensures a stable convergence of the problem.

4 | DISCONTINUOUS GALERKIN METHOD

To numerically solve the partial differential equations associated with the **H**-formulation, we will discretize them over the domain Ω using the interior penalty discontinuous Galerkin method.[7] This method combines numerical approaches of both the finite element method and the finite volume method.

The discretization will rely on the same mesh as defined above in the finite element method. Appropriate interface terms will be derived based on the symmetric interior penalty method to ensure the magnetic field continuity and convergence.[10]

4.1 | Discrete variational formulation

The discontinuous Galerkin discretization of Equation 4 will need a nodal approximation $\mathbf{u}^h$ of the unknown magnetic field **H**. The approximated field $\mathbf{u}^h$ will be defined over each finite element K. It will belong to the following finite element space:

$$\mathbf{W}^h = \left\{\mathbf{w} \in (\mathbf{L}^2(\Omega))^3 \,:\, \mathbf{w}|_K \in (\mathbb{P}^m(K))^3, K \in \mathcal{T}_h\right\} \tag{13}$$

with $\mathbb{P}^m(K)$ the set of polynomials of total degree at most m on K.

The discrete weak formulation of Equation 4 on each element K will consist in finding $\mathbf{u}^h \in \mathbf{W}^h$ such that

$$\begin{aligned}&\sum_{K\in\mathcal{T}_h} \int_K \mathbf{u}_t^h \cdot \boldsymbol{\varphi} dK + \sum_{K\in\mathcal{T}_h} \int_K \kappa \cdot \mathrm{curl}\mathbf{u}^h \cdot \mathrm{curl}\boldsymbol{\varphi} dK \\ &\qquad + I_h = \mathbf{0}, \;\; \forall \boldsymbol{\varphi} \in \mathbf{W}^h\end{aligned} \tag{14}$$

with $\mathbf{u}_t^h = \partial \mathbf{u}^h / \partial t$, $\kappa = \rho/\mu_0$ and the interface term $I_h = -\sum_{K\in\mathcal{T}_h} \int_{\partial K} ((\kappa \cdot \mathrm{curl}\mathbf{u}^h) \times \mathbf{n}) \cdot \boldsymbol{\varphi} dA$ where $\mathbf{n}$ is the interface normal vector.

The formulation above uses tools of the finite element method. It specifically approximates the weak formulation of the H-formulation partial differential equations locally on each element K. However, the finite volume method has not been implemented.The continuity of both the normal and tangential components of the magnetic field **H** is also not considered.

Thus, the finite volume method implementation must ensure the continuity of the magnetic field **H** at each face of Γ_h to fully respect Maxwell equations.

4.2 | Numerical fluxes term on the faces of the mesh $\mathcal{T}_h$

The finite volume method approach will help us construct new interfaces terms expressed as numerical fluxes. The derived term, based on the symmetric interior penalty method, should be equivalent to I_h. It must ensure the continuity of the normal and tangential components of the magnetic field **H** across each face $f \in \mathcal{T}_h$. The face will either belong to 2 neighbouring elements K and K' as $f = \partial K \cap \partial K'$ or to the boundary Γ as $f = \partial K \cap \Gamma$.

Grote was able to derive error estimates from the use of the interior penalty discontinuous Galerkin method

applied to Maxwell equations.[10] He proposed an equivalent interface term function of the electric field or the magnetic field and based on the symmetric interior penalty method.

His proposed interface term applied to the **H**-formulation will be expressed as follows:

$$\begin{aligned} &-\sum_{f\in\Gamma_h}\int_f[\boldsymbol{\varphi}\times\mathbf{n}]\cdot\{\{\kappa\cdot\mathrm{curl}\mathbf{u}^h\}\}dA \\ &-\sum_{f\in\Gamma_h}\int_f[\mathbf{u}^h\times\mathbf{n}]\cdot\{\{\kappa\cdot\mathrm{curl}\boldsymbol{\varphi}\}\}dA+I_h^p \end{aligned} \tag{15}$$

with the penalty term $I_h^p=\sum_{f\in\Gamma_h}\int_f \mathtt{a}\cdot[\mathbf{u}^h\times\mathbf{n}]\cdot[\boldsymbol{\varphi}\times\mathbf{n}]dA$.

The quantities $[\mathbf{u}^h\times\mathbf{n}]$ and $\{\{\mathbf{u}^h\times\mathbf{n}\}\}$ denote the jump and average of the tangential components of the field $\mathbf{u}^h$ across each face f. For instance, if $f=\partial K\cap\partial K'$ for 2 neighbouring elements K and K', the respective jump and average of the tangential components of the magnetic field are as follows:

$$\{\{\mathbf{u}^h\times\mathbf{n}\}\}=\mathbf{u}_K^h\times\mathbf{n}-\mathbf{u}_{K'}^h\times\mathbf{n} \tag{16}$$

and

$$[\mathbf{u}^h\times\mathbf{n}]=\frac{\mathbf{u}_K^h\times\mathbf{n}+\mathbf{u}_{K'}^h\times\mathbf{n}}{2}. \tag{17}$$

In the penalty term I_h^p, function $\mathtt{a}$ penalizes the jump of the tangential components of the fields $\mathbf{u}^h$ and $\boldsymbol{\varphi}$. According to Grote, it is defined as follows:

$$\mathtt{a}|_f=\alpha\mathtt{mh} \tag{18}$$

with

$$\mathtt{m}|_f=\begin{cases}\max(\kappa_K,\kappa_{K'}), & f=\partial K\cap\partial K'\\ \kappa_K, & f=\partial K\cap\Gamma\end{cases} \tag{19}$$

and

$$\mathtt{h}|_f=\begin{cases}\max(h_K,h_{K'}), & f=\partial K\cap\partial K'\\ h_K, & f=\partial K\cap\Gamma\end{cases}. \tag{20}$$

The coefficient α is a constant whose minimum value must depend on the shape-regularity of the mesh and the approximation order of the field $\mathbf{u}^h$. The larger α becomes, the smaller the time step will be for the solver to reach convergence.

However, the interface term expression defined above is difficult to implement numerically. To ease this process, the interface term must be rewritten in terms of fluxes, as derived by the finite volume method, projected on the basis vector function $\boldsymbol{\varphi}$.

First, the following mixed product invariance property:

$$\mathbf{a}\cdot(\mathbf{b}\times\mathbf{c})=\mathbf{b}\cdot(\mathbf{c}\times\mathbf{a})=\mathbf{c}\cdot(\mathbf{a}\times\mathbf{b}) \tag{21}$$

with vectors $\mathbf{a}$, $\mathbf{b}$, and $\mathbf{c}$, applied in Equation 15 whose first term has $\mathbf{a}=\kappa\cdot\mathrm{curl}\mathbf{u}^h$, $\mathbf{b}=\boldsymbol{\varphi}$, $\mathbf{c}=\mathbf{n}$ while the second term has $\mathbf{a}=\mathbf{u}^h\times\mathbf{n}$, $\mathbf{b}=\kappa\cdot\nabla$ and $\mathbf{c}=\boldsymbol{\varphi}$. It will lead to the interface term expression below:

$$\begin{aligned} &\sum_{f\in\Gamma_h}\int_f[\boldsymbol{\varphi}]\cdot\{\{(\kappa\cdot\mathrm{curl}\mathbf{u}^h)\times\mathbf{n}\}\}dA \\ &\qquad+\sum_{f\in\Gamma_h}\int_f[(\kappa\cdot\mathrm{curl}\mathbf{u}^h)\times\mathbf{n}]\cdot\{\{\boldsymbol{\varphi}\}\}dA+I_h^p. \end{aligned} \tag{22}$$

The penalty term $I_h^p=-\sum_{f\in\Gamma_h}\int_f \mathtt{a}\cdot[\boldsymbol{\varphi}]\cdot[\mathbf{n}\times\mathbf{u}^h\times\mathbf{n}]dA$.

While this expression showcases projections on the basis vector function $\boldsymbol{\varphi}$, it does not introduce fluxes quantities. Fluxes will be introduced in Equation 22 by rewriting the curl-curl operator as a divergence operator div. The equivalence of both operators is derived below:

$$\kappa\cdot\mathrm{curl}\mathbf{u}^h=(F_x^h,F_y^h,F_z^h), \tag{23}$$

and

$$\mathbf{F_1}=(0,F_z^h,-F_y^h),\mathbf{F_2}=(-F_z^h,0,F_x^h),\mathbf{F_3}=(F_y^h,-F_x^h,0) \tag{24}$$

will give the following derivations

$$\begin{cases}\mathrm{curl}(\kappa\cdot\mathrm{curl}\ \mathbf{u}^h)=(\mathrm{div}\ \mathbf{F_1},\mathrm{div}\ \mathbf{F_2},\mathrm{div}\quad\mathbf{F_3})\\ (\kappa\cdot\mathrm{curl}\mathbf{u}^h)\times\mathbf{n}=(\mathbf{F}_1\cdot\mathbf{n},\mathbf{F}_2\cdot\mathbf{n},\mathbf{F}_3\cdot\mathbf{n})\end{cases}. \tag{25}$$

Vectors $\mathbf{F_1},\mathbf{F_2}$, and $\mathbf{F_3}$ are fluxes quantities. By combining the above derivations with the interface term expression (22), the final interface term, expressed as numerical fluxes, is the following:

$$\sum_{f\in\Gamma_h}\sum_{i=1}^{3}\int_f[\varphi_i]\cdot\{\{\mathbf{F}_i\cdot\mathbf{n}\}\}dA+\sum_{f\in\Gamma_h}\sum_{i=1}^{3}\int_f[\mathbf{F}_i\cdot\mathbf{n}]\cdot\{\{\varphi_i\}\}dA+I_h^p, \tag{26}$$

where the penalty term I_h^p remains unchanged.

4.3 | Numerical treatment of the non-linearities arising from $\mathbf{E}=\rho(\mathbf{J})\mathbf{J}$

Unlike the finite element implementation, the discontinuous Galerkin method will allow, with its local approximation of the problem on each element, either an explicit or an implicit treatment of the non-linear resistivity $\rho(\mathbf{J})$ of the problem. A linearization of the power law in such method will be explored in another paper.

In the explicit case, the resistivity ρ^{l-1} , evaluated at the time step t_p^{l-1} of the problem resolution, will be used as an input in the problem at following time step t_p^l.

In the implicit case, the full expression of the resistivity ρ will be included in the problem definition. Internally, a Newton-Raphson algorithm will ensure a good approximation of ρ at each time step t_p^l of the problem resolution.

The convergence, once reached in each approach, will give a good enough approximation of the solution.

5 | NUMERICAL RESULTS

5.1 | Superconducting cube subjected to an external magnetic field

A superconducting cube of 2 mm side length, subjected to an external magnetic field $\mathbf{H_a}$ oriented in the y-direction, will be modeled in three dimensions using both numerical methods mentioned above. Comparisons of the computed AC losses, over a period, using both methods will help us validate them.

The superconducting behaviour of the cube is characterized by a critical electric field $E_c = 10^{-7}V/mm$, a critical current density $J_c = 100A/mm^2$ and a power law exponent $n = 10$. The magnetic field $\mathbf{H_a} = H_m sin(2\pi ft)\mathbf{e_y}$, with a magnetic flux density amplitude $B_m = 0.1\,T$ and a frequency $f = 50\,Hz$, will be applied on the external boundary of a less conductive domain.

The resistivity $\rho_{r,a}$ of such domain will be set close enough to the air resistivity. The goal is to be able to model a non-conductive domain such that the correct total magnetic field is applied on the boundaries of the superconducting cube. The resistivity of such domain has been set at $10^{-3}\Omega.m$. Moreover, the domain has been defined as a cube of side length 4 mm that surrounds the superconducting cube.

In this problem, both numerical methods implementation used the same meshed domain of 15948 tetrahedra. However, computations with the finite element method were done on a single processor while the discontinuous Galerkin method used 16 processors. As illustrated in Figure 1, the current density has also been computed and it shows good agreement with the physics characterizing the problem.

As shown in Figure 2, the computed AC losses are quite similar for both the finite element and the discontinuous Galerkin. However, the major difference between both methods lies in the computation time. For this example, the overall computation time, with a time step of 25 milliseconds, was 30 minutes for the discontinuous Galerkin method and about 2 hours for the finite element method.

In the case of the discontinuous Galerkin method, parallel computations are naturally implemented and they enable the scaling of both the problem matricial system and the meshed domain over numerous processors. Such advantages remove memory limitations encountered in large scale-problems modeled in 3D using finite element method. Those limitations are mostly due to the size of the meshed domain.

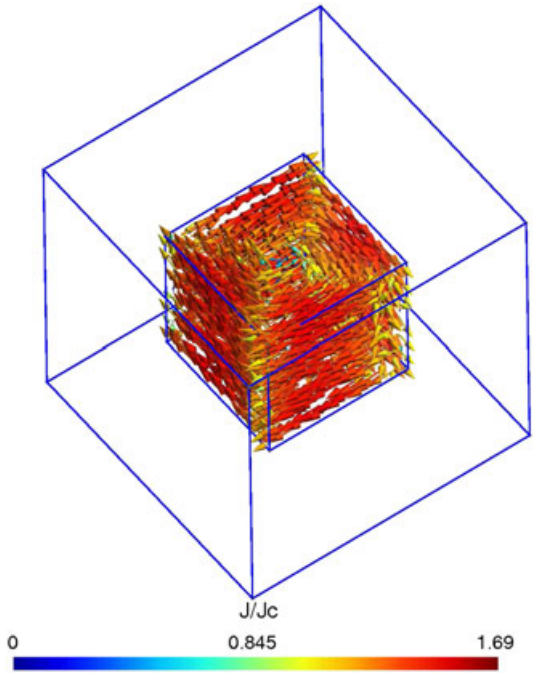

FIGURE 1 Computed current distribution inside the superconducting cube using the discontinuous Galerkin method

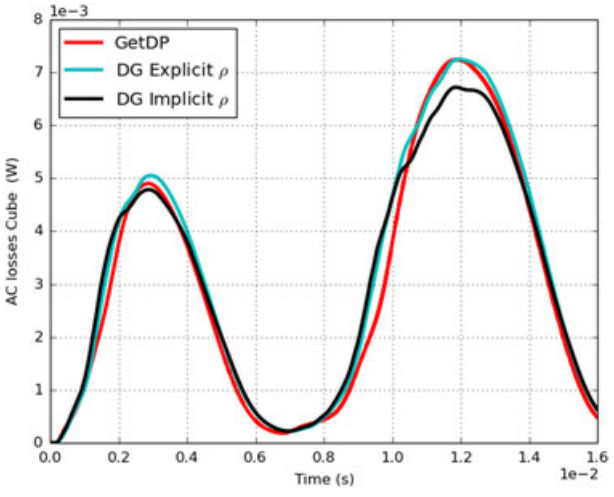

FIGURE 2 Total AC losses of a superconducting cube subjected to an external magnetic field computed over T with GetDP and the discontinuous Galerkin (DG) method with the non-linear resistivity evaluated explicitly and implicitly

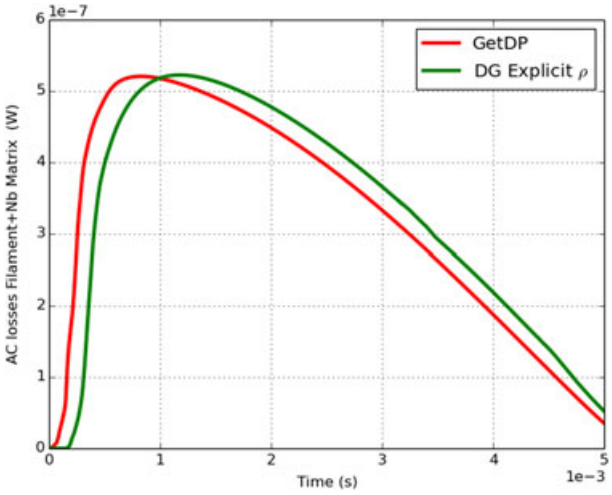

FIGURE 3 Total AC losses of a superconducting filament inside a niobium matrix subjected to a transverse external magnetic field computed over $T/4$ with GetDP and the discontinuous Galerkin method with the non-linear resistivity evaluated explicitly

5.2 | Superconducting filament inside a resistive matrix subjected to a transverse external magnetic field

A superconducting filament inside a resistive matrix, with a 2.63 mm length and respective radiuses of 36 and 0.33 mm, subjected to a transverse external magnetic field $\mathbf{H_a}$, will be modeled using both numerical methods mentioned above. Comparisons of the computed AC losses, over a quarter of period, using both methods will be done.

The superconducting behaviour of the filament is characterized by the same properties values as the cube modeled above, except the power law exponent value, which is $n = 20$. The magnetic field $\mathbf{H_a}$, similar to the cube model, will also be applied on the external boundary of a less conductive domain.

Although the resistivity of this domain remains the same as the one defined in the previous application, the domain geometry is now a cylinder, with a 0.5-mm radius and a 3.03-mm length. It surrounds the system that consists of a superconducting filament inside a niobium matrix of conductivity $6.10^9 S.m^{-1}$.

Computations with the finite element method were still done on a single processor while the discontinuous Galerkin method used 16 processors.

As shown in Figure 3, the computed AC losses, for both the finite element and the discontinuous Galerkin, are still in good agreement.

6 | CONCLUSION

A nodal discontinuous Galerkin method has been proposed to model high-temperature superconductors in three dimensions. It solves efficiently 3D non-linear dynamic magnetic problems, combining the **H**-formulation and the non-linear electrical behaviour of high-temperature superconductors. Numerical fluxes were appropriately defined, using the symmetry interior penalty method, to ensure the continuity of the tangential component of the magnetic field across each interface of the studied mesh. Because of the local approximation of the problem on each element brought by the method, the non-linearities are dealt with an evaluation, either explicitly or implicitly, of the superconductors resistivity. A linearisation of the power law, implemented in the finite element method to stabilize the convergence, has not been explored yet. Comparisons on simple applications, with the finite element method implemented with GetDP, show good agreement in terms of computed AC losses. Moreover, parallel computations, naturally geared for the discontinuous Galerkin method, remove memory limitations. Thus, this method provides, with the use of GPU-accelerated computations for instance, a good framework for fast and efficient computations of highly non-linear superconductivity problems in three dimensions. An extended use of this method for the modeling of thermal-electromagnetic problems related to superconductors and multifilamentary superconducting wires is in progress.

ORCID

L. Makong http://orcid.org/0000-0002-5510-008X

REFERENCES

1. Masson PJ, Soban DS, Upton E, Pienkos JE, Luongo CA. HTS motors in aircraft propulsion: design considerations. *IEEE Trans Appl Supercond*. 2005;15(2):2218-2221.
2. Chen SD, Yu YT, Huang ZW, et al. Design of a HTS magnet for application to resonant X-ray scattering. *IEEE Trans Appl Supercond*. 2013;21(3):1661-1664.
3. Zeldov E, Amer NM, Koren G, Gupta A, McElfresh MW, Gambino RJ. Flux creep characteristics in high temperature superconductors. *Appl Phys Lett*. 1990;56(7):680-683.
4. Grilli F, Stavrev S, Le Floch Y. Finite-element method modeling of superconductors: From 2-D to 3-D. *IEEE Trans Appl Supercond*. 2005;15(1):17-25.
5. Grilli F, Brambilla R, Sirois F, Stenvall A, Memiaghe S. Development of a three-dimensional finite-element model for high-temperature superconductors based on the H-formulation. *Cryogenics*. 2013;53:142-147.
6. Sirois F, Grilli F. Potential and limits of numerical modelling for supporting the development of HTS devices. *Supercond Sci Technol*. 2015;28(4):043002-043014.
7. Arnold DN, Brezzi F, Cockburn B, Marini LD. Unified analysis of discontinuous Galerkin methods for elliptic problems. *SIAM J Numer Anal*. 2002;39(5):1749-1779.
8. Kameni A, Boubekeur M, Alloui L, Bouillault F, Lambrechts J, Geuzaine C. A 3-D semi-implicit method for computing the

current density in bulk superconductors. *IEEE Trans Magn*. 2014;50(2):377-380.

9. Makong L, Kameni A, Masson P, Lambrechts J, Bouillault F. 3-D modeling of heterogeneous and anisotropic superconducting media. *IEEE Trans Magn*. 2005;52(3):1-4.
10. Grote M, Schneebeli A, Schzau D. Interior penalty discontinuous Galerkin method for Maxwells equations: energy norm error estimates. *J Comput Appl Math*. 2007;204:375-386.
11. http://onelab.info/wiki/Superconducting_wire.

How to cite this article: Makong L, Kameni A, Bouillault F, Geuzaine C, Masson P. Nodal discontinuous Galerkin method for high-temperature superconductors modeling based on the H-formulation. *Int J Numer Model*. 2018;31:e2298. https://doi.org/10.1002/jnm.2298